Photochemical & Photobiological Sciences

Dynamic Article Links

Cite this: *Photochem. Photobiol. Sci.*, 2012, **11**, 979

www.rsc.org/pps

PAPER

Characterization and reactivity of photodimers of dihydroneopterin and dihydrobiopterin†‡

Mariana Vignoni,[a] Carolina Lorente,[a] Franco M. Cabrerizo,[b] Rosa Erra-Balsells,[c] Esther Oliveros*[d] and Andrés H. Thomas*[a]

Received 3rd November 2011, Accepted 9th December 2011
DOI: 10.1039/c2pp05363b

7,8-Dihydrobiopterin (H_2Bip) and 7,8-dihydroneopterin (H_2Nep) belong to a class of heterocyclic compounds present in a wide range of living systems. H_2Bip accumulates in the skin of patients suffering from vitiligo, whereas H_2Nep is secreted by human macrophages when the cellular immune system is activated. We have investigated the photochemical reactivity of both compounds upon UV-A irradiation (320–400 nm), the chemical structures of the products and their thermal stability. The study was performed in neutral aqueous solutions. The reactions were followed by UV/Visible spectrophotometry and HPLC and the products were analyzed by means of electrospray ionization mass spectrometry and ^{1}H-NMR. Excitation of H_2Bip and H_2Nep leads to the formation, in each case, of two main isomeric dimers. The latter compounds undergo a thermal process that may consist in a retro [2 + 2]-cycloaddition and hydrolysis to yield the reactant (H_2Bip or H_2Nep) and a product that has incorporated a molecule of H_2O.

1 Introduction

Pterins, heterocyclic compounds widespread in biological systems, are derived from 2-aminopteridin-4(1*H*)-one[1] and play different roles ranging from pigments to enzymatic cofactors for numerous redox and one-carbon transfer reactions.[2,3] Pterins are synthesized *in vivo* by the cleavage of guanosine 5′-triphosphate. The first intermediate of the biosynthetic pathway, 7,8-dihydroneopterintriphosphate is either converted to 7,8-dihydroneopterin (H_2Nep) and neopterin (Nep) or to 5,6,7,8-tetrahydrobiopterin (H_4Bip).[4] From a biological point of view, biopterin (Bip) and neopterin, and their 7,8-dihydro and 5,6,7,8-tetrahydro derivatives (denoted throughout as dihydropterins and tetrahydropterins, respectively) are probably the most important unconjugated pterins (Scheme 1).

H_2Nep and Nep are secreted by human macrophages upon stimulation with interferon-γ.[5,6] When the cellular immune system is activated, the concentration of Nep increases in body fluids and, consequently, measurement of its concentrations allows to sensitively monitor the degree of immune activation.[7,8] For instance, high levels of Nep are particularly apparent during infections caused by viruses and intracellular bacteria and parasites.[9] H_4Bip is involved in the metabolism of amino acids[10] and is present in the skin of human beings acting as a cofactor of phenylalanine hydroxylase, an enzyme that catalyzes the oxidation of phenylalanine to tyrosine. This latter amino acid is the precursor of melanin, the pigment of human skin and the main natural protection against the harmful effects of UV radiation.

Dihydrobiopterin (H_2Bip), Bip, which has been demonstrated to be toxic for melanocytes,[11] and other pterin derivatives (Scheme 1) accumulate in the skin of patients suffering from vitiligo,[12,13] a chronic depigmentation disorder. In the tissues affected by this disease, hydrogen peroxide (H_2O_2) is present in high concentrations and the cells undergo oxidative stress, deactivation of enzymes of the melanin biosynthesis takes place and the protection of the skin against UV radiation fails because of the lack of melanin. Therefore, the photochemistry of pterins is of particular interest for the study of this disease. Moreover, 6-carboxypterin (Cap), a product of Bip photolysis that is not synthesized in the skin cells, has been isolated from the affected skin,[14] thus proving that photooxidation of pterins occurs *in vivo* under pathological conditions. Upon UV-A irradiation (320–400 nm), oxidized pterins produce reactive oxygen

[a]*Instituto de Investigaciones Fisicoquímicas Teóricas y Aplicadas (INIFTA), Departamento de Química, Facultad de Ciencias Exactas, Universidad Nacional de La Plata, CCT La Plata-CONICET, Casilla de Correo 16 Sucursal 4, (1900) La Plata, Argentina. E-mail: athomas@inifta.unlp.edu.ar; Fax: +54 221 4254642*
[b]*Instituto de Investigaciones Biotecnológicas-Instituto Tecnológico de Chascomús (IIB-INTECH), Universidad Nacional de San Martín, CONICET, Intendente Marino Km 8.2 CC 164, (7130) Chascomús, Argentina*
[c]*CIHIDECAR-CONICET, Departamento de Química Orgánica, Facultad de Ciencias Exactas y Naturales, Universidad de Buenos Aires, Pabellón 2 3p Ciudad Universitaria, 1428 Buenos Aires, Argentina*
[d]*Laboratoire des Interactions Moléculaires et Réactivité Chimique et Photochimique (IMRCP), UMR CNRS 5623, Université Paul Sabatier (Toulouse III), 118 route de Narbonne, F-31062 Toulouse cédex 9, France. E-mail: oliveros@chimie.ups-tlse.fr; Fax: +33 5 61558155*

† This article is published as part of a themed issue in honour of Professor Kurt Schaffner on the occasion of his 80th birthday.

‡ Electronic supplementary information (ESI) available. See DOI: 10.1039/c2pp05363b

R	7,8-Dihydropterin	5,8-Dihydropterin	Oxidized pterin
	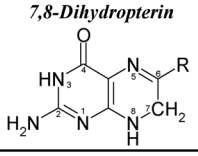	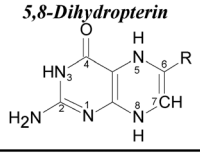	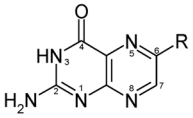
-C_αHOH-C_βHOH-$C_\gamma H_2$OH	Dihydroneopterin (H_2Nep)	5,8-Dihydroneopterin (5,8-H_2Nep)	Neopterin (Nep)
-C_αHOH-C_βHOH-$C_\gamma H_3$	Dihydrobiopterin (H_2Bip)	5,8-Dihydrobiopterin (5,8-H_2Bip)	Biopterin (Bip)

Scheme 1 Chemical structures of some pterin derivatives mentioned in this work.

species, such as singlet oxygen ($^1O_2$),[15] superoxide anion ($O_2^{\cdot-}$)[16] and H_2O_2,[17] and are able to photoinduce oxidation of DNA and its components.[18,19] Therefore, accumulation of oxidized pterins in the skin enhances the harmful effects of UV radiation and very likely contributes to the oxidative stress in vitiligo.

Very recently, the photochemistry of H_2Bip[20] and H_2Nep[21] in aqueous solution upon UV-A irradiation was described. Briefly, it has been suggested that excitation of both compounds leads to the formation of isomeric dimers. These photodimerizations are independent of the O_2 concentration and take place from the singlet excited state of the reactant. The corresponding quantum yields were determined to be $(5.3 \pm 0.3) \times 10^{-2}$ and $(3.8 \pm 0.5) \times 10^{-2}$ for H_2Bip and H_2Nep, respectively. Apart from the photodimerization, in the presence of O_2, H_2Bip is converted into its oxidized analogue (Bip) and this reaction has been considered as a potential source of Bip in the skin. This oxidative pathway does not occur in the case of H_2Nep. Finally for both compounds non fully characterized products were reported.

In the context of our investigations on the photochemistry of pterins, we have performed in this work new analyses on the structure of the photoproducts of H_2Bip and H_2Nep, and a kinetic study of their thermal stability. In particular, we confirmed by high resolution mass spectrometry and ^{1}H-NMR the dimeric nature of the main photoproducts resulting from a [2 + 2]-cycloaddition, and showed that they decompose in the dark regenerating partially the dihydropterin.

2 Experimental

2.1 Chemicals

H_2Nep, H_2Bip and other pterins were purchased from Schircks Laboratories (Switzerland) and used without further purification. Other chemicals were from Sigma Chemical Co. The pH of the aqueous solutions was adjusted by adding drops of HCl or NaOH solutions from a micropipette. The concentrations of the acid and base used for this purpose ranged from 0.1 to 2 M. The ionic strength was approximately 10^{-3} M in all the experiments.

2.2 Steady-state irradiation

The continuous photolysis of 7,8-dihydropterins aqueous solutions was carried out in quartz cells (1 cm optical pathlength) at room temperature. Two radiation sources were employed: (I) Rayonet RPR lamps emitting at 350 nm (Southern N.E. Ultraviolet Co.) and (II) Xe/Hg Osram 1000 W with a monochromator ISA Jobin-Yvon B204. Irradiation experiments were performed in the presence and in the absence of air. Deaerated solutions were obtained by bubbling with Ar gas for 20 min.

2.3 UV/Visible spectrophotometric analysis

Electronic absorption spectra were recorded on diode array spectrophotometers 8452A and 8453 (Hewlett Packard) or Shimadzu UV-1800. Measurements were made using quartz cells of 0.4 or 1 cm optical path length. The absorption spectra of the solutions were recorded at regular time intervals during irradiation.

2.4 High performance liquid chromatography

Two chromatographic systems were employed for monitoring the reaction: I) a Prominence equipment from Shimadzu (photodiode array detector SPD-M20A) with a Synergy Polar-RP column (150 × 4.6 mm, 4 μm, Phenomenex); II) a Waters Alliance equipment (photodiode array detector Waters 996) with an XTerra RP18 column (250 × 4.6 mm, 5 μm, Waters). The mobile phase consisted of 0–4% of methanol and 100–96% of an aqueous solution containing 10 mM ammonium acetate (pH = 7). Aqueous solutions of commercial standards were employed for obtaining calibration curves of reactants and products.

2.5 Mass spectrometry analysis

Two LC/MS systems were employed for analyzing the products. Equipment I was used for the exact mass measurements and consisted of a Q TOF Ultima API (Waters) coupled to an HPLC chromatograph (Waters). Equipment II consisted of a triple quadrupole mass spectrometer (Q TRAP Applied Biosystems), equipped with electrospray ion (ESI) source (Turbo Ion Spray (TIS)) coupled to an HPLC chromatograph (Agilent 1100). Both HPLC analyses were performed by using a XTerra RP18 column (*vide supra*), and isocratic elution with 96% ammonium acetate (10 mM) and 4% methanol at a flow rate of 0.6 mL min^{-1}.

2.6 Nuclear magnetic resonance (NMR)

^{1}H-NMR spectra of irradiated and non-irradiated H_2Bip and H_2Nep solutions were recorded on a Bruker AM-500 spectrometer operating at 500 MHz. D_2O was used as a solvent and the chemical shift of H_2O (4.79 ppm with respect to tetramethylsilane) was used as an internal reference. In order to improve the

signal-to-noise ratio, a selective NMR irradiation of the H_2O peak was performed while recording the ^{1}H-NMR spectra of the sample under study. Typically, solutions were introduced into a 5 mm diameter tube. The acquisition parameters were: spectral width 7500 Hz, relaxation delay 3 s, number of scans 32–64, acquisition time 4.369 s. The experiments were carried out at 300 K. ^{1}H-NMR spectra of H_2Bip and H_2Nep are given below (chemical shifts δ in ppm, coupling constants J in Hz).

^{1}H-NMR spectrum of H_2Bip. The ^{1}H-NMR spectrum of H_2Bip in D_2O showed four proton signals at low δ values with relative intensities (measured as the integral of each peak) of 2 : 1 : 1 : 3 (δ = 4.18 (dd, J_{gem} = 0.5), 4.09 (d, $J_{\alpha,\beta}$ = 6), 3.99 (m) and 1.21 (d, $J_{\beta,\gamma}$ = 6.5)). D_2O only allows detecting non-interchangeable proton signals. Therefore, detected signals would correspond to axial and equatorial protons at C(7) (not-well resolved signals that appear in a quite close region of the NMR spectra) and to protons on the aliphatic chain substituent at C(6) (H_α, H_β and H_γ), respectively (Fig. 1S, ESI‡).

^{1}H-NMR spectrum of H_2Nep. The spectrum of H_2Nep[22] presents some differences in the NMR pattern compared to H_2Bip, mainly due to the difference in the aliphatic chain (Scheme 1). In this case, four groups of signals with relative intensities 3 : 1 : 1 : 1 can be distinguished. A group corresponding to three protons appears in the δ region of 4.19–4.23 ppm. Taking into account the broadness and the distortion of the signals, they can be assigned to overlapping signals of axial and equatorial protons at C(7) ($\delta = 4.21_4$, two poorly resolved doublets) and H_α ($\delta = 4.20_8$ (d, $J_{\alpha,\beta}$ = 6)). Other signals have δ values of 3.88 (m), 3.78 (dd, $J_{\beta,\gamma a}$ = 3.5, $J_{\gamma a,\gamma b}$ = 12) and 3.65 (dd, $J_{\beta,\gamma b}$ = 6.5, $J_{\gamma a,\gamma b}$ = 12). As previously reported in the literature,[22] the latter signals were assigned to the H_β methine proton and to the $H_a\gamma$ and $H_b\gamma$ methylene protons of H_2Nep, respectively.

2.7 Molecular modeling

The ground state geometries were calculated with the semi-empirical parametrized AM1 and PM3 methods as implemented in the software HyperChem 8.0.7 for Windows (Restricted Hartree–Fock (RHF) formalism; total charge: 0; spin multiplicity: 1; convergence limit: $1e^{-8}$; iteration limit: 50; accelerated convergence: on; CI method: none; Polak-Ribiere algorithm; RMS gradient: 0.006 kcal Å^{-1} mol^{-1}; *in vacuo*). PM3 has proved to be effective in studies of aromatic molecules containing heteroatoms, compared with other methods such as MINDO/3 or MNDO. Molecule dipole moment values were calculated at the ZINDO/S level.

3 Results and discussion

3.1 Photolysis of H_2Nep and H_2Bip: Mass spectrometry analysis

The photolysis experiments were carried out in Ar-saturated and air-equilibrated solutions (pH 7.0) for H_2Nep. In the case of H_2Bip however, experiments were only performed in Ar-saturated solutions (pH 7.0), as this dihydropterin undergoes a photosensitized reaction leading to Bip in the presence of O_2.[20] For both compounds, the irradiation-induced spectral changes were consistent with previous studies:[20,21] the characteristic low energy band of dihydropterins decreased in intensity, whereas an increase in the absorbance at 240–250 nm was observed. Likewise, the HPLC analysis was also similar to that previously reported: (i) 3 photoproducts (P1, P2 and P3), with retention times lower than that of the reactant, were formed; (ii) the areas of the peaks (λ_{AN} = 270 nm) corresponding to P2 and P3 were similar and much larger than that corresponding to P1; (iii) the spectra of the photoproducts P2 and P3 were also quite similar, with no absorption above 320 nm and a band centered at 246 nm. Analysis by electrospray ionization mass spectrometry (ESI-MS) previously suggested that P2 and P3 are isomeric dimers.[20]

In this work, the solutions of H_2Bip and H_2Nep were analyzed, before and after irradiation (source II, 335 nm, Experimental Section), by HPLC coupled to a high resolution mass spectrometer (HRMS) in positive mode (Equipment I, Experimental section). In non-irradiated solutions, the signals corresponding to the intact molecular ions of H_2Bip and H_2Nep as $[M + H]^+$ species at *m/z* 240.1781 and 256.2732 were observed, respectively. These *m/z* values correspond to the elemental compositions of H_2Bip ($C_9H_{13}N_5O_3$ + H) and H_2Nep ($C_9H_{13}N_5O_4$ + H), respectively.

Analysis of irradiated solutions of H_2Bip shows that the more intense peaks of the mass spectra of P2 and P3 are identical, and correspond to the mass of the intact protonated molecular ion of H_2Bip ($[M + H]^+$). However, both P2 and P3 have an additional peak at *m/z* = 479.2098, which corresponds to $[M_2 + H]^+$ and results in an elemental composition of $C_{18}H_{26}N_{10}O_6$ + H with a mass error of −1.7 mDa. Similar results were obtained for H_2Nep: (i) the more intense peaks of the mass spectra of P2 and P3 are identical and correspond to the mass of the intact ion of H_2Nep ($[M + H]^+$); (ii) both P2 and P3 have an additional peak at *m/z* = 511.2026, which corresponds to $[M_2 + H]^+$ and results in an elemental composition of $C_{18}H_{26}N_{10}O_8$ + H with a mass error of −1.3 mDa. This analysis confirmed that P2 and P3 are dimers in the case of both H_2Bip and H_2Nep. Furthermore the presence of the signals at *m/z* = $[M + H]^+$ suggests that the dimers easily suffer fragmentation (decomposition).

Product P1 could not be analyzed with Equipment I (Experimental section) because it migrated with the solvent front, under all the different chromatographic conditions assayed. Therefore no information about the exact molecular weight of this compound was obtained under our analytical conditions. However, P1 obtained for H_2Bip could be analyzed using equipment II (Experimental section). A molecular ion of *m/z* = 258 was obtained for P1, corresponding to the mass of $[H_2Bip + H_2O + H]^+$ = [239 + 18 + 1] and thus suggesting that P1 could correspond to a molecule of H_2Bip that has incorporated an H_2O molecule.

3.2 Thermal stability of the photodimers

The stability of the dimers (P2 and P3) and of product P1 was studied in a series of experiments in which O_2-free solutions (pH 7.0) of H_2Bip and H_2Nep were irradiated (source II, 350 nm, Experimental section), and then kept in the dark for

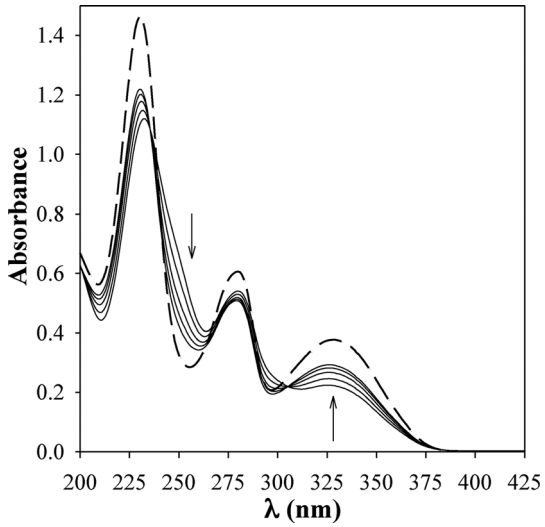

Fig. 1 Evolution of the absorption spectrum of an aqueous solution of H_2Nep ($[H_2Nep]_0$ = 150 μM, pH = 7.0) as a function of time after irradiation was stopped. Spectra were recorded at 1, 60, 135, 210 and 315 min after interrupting the irradiation (6 min at 350 nm); dashed line: spectrum of H_2Nep before irradiation.

different times before being analyzed by UV/visible spectrophotometry, HPLC and H_2O_2 determination. To evaluate the role of O_2 in the studied processes some solutions were aerated immediately after interrupting the irradiation.

For both reactants, absorption spectra changed as a function of time after interrupting the irradiation, suggesting that the photoproducts underwent thermal reactions. The characteristic low energy band of dihydropterins increased ($\lambda_{max} \sim 330$ nm), whereas a decrease in the absorbance at 250 nm was observed (Fig. 1). Besides, in comparative experiments carried out keeping in the dark irradiated air-equilibrated and free-O_2 solutions, similar results were obtained, *i.e.*, the difference spectra registered for a given time were equal, within the experimental error, for both experimental conditions, thus suggesting the thermal process is O_2-independent.

HPLC analysis revealed that after interrupting the irradiation the areas of the peaks corresponding to the dimers decreased, whereas the area of the peaks corresponding to P1 and the reactant (H_2Bip or H_2Nep) increased (Fig. 2). In agreement with spectral analysis, the same behavior was observed for O_2-free and air-equilibrated solutions. In addition, H_2O_2 was investigated during the process and no formation of this reactive oxygen species was detected. The results suggest that after photochemical formation, the dimers undergo a thermal process to yield the reactant (H_2Bip or H_2Nep) and P1. Taking into account that the analysis by mass spectrometry for H_2Bip showed that the molecular mass of P1 corresponds to [H_2Bip + H_2O] (*vide supra*), the HPLC results suggest that the thermal degradation of dimers might be due to a retro [2 + 2]-cycloaddition reaction and hydrolysis and, in this process, one of the monomers incorporates a molecule of H_2O.

To further investigate this process, a series of experiments at different initial concentrations of reactants (R = H_2Bip or H_2Nep) and irradiation times were carried out. For each photolysis, the irradiated solutions were kept in the dark until no spectral

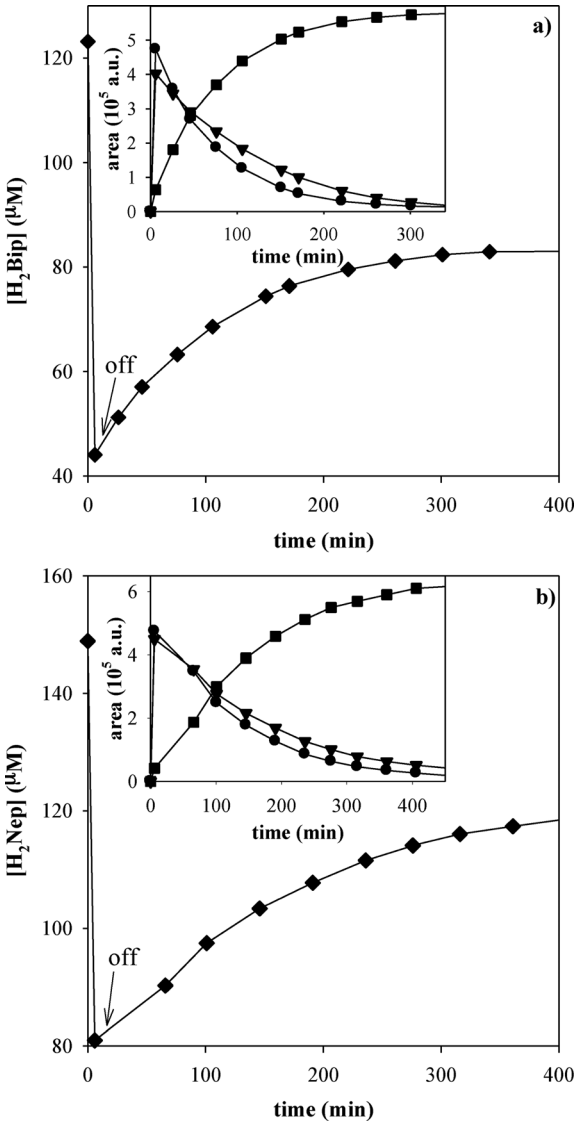

Fig. 2 Concentrations profiles of the dihydropterins investigated during the thermal decomposition of the dimers (chromatographic system I). At t = 0, the irradiation was started and at t = 6 min (arrow) the irradiation was stopped. (a) $[H_2Bip]_0$ = 123 μM, pH = 6.5, irradiated under anaerobic conditions; (b) $[H_2Nep]_0$ = 150 μM, pH = 7.0, irradiated in air-equilibrated solution. Insets: time evolution of the area of the chromatographic peaks corresponding to dimers P2 and P3 (circles and triangles, analysis at 270 nm) and to P1 (squares, analysis at 250 nm).

changes were observed anymore; *i.e.* the thermal degradation of the dimers (D) was complete (t > 5 h). Then the consumption of R in the photochemical reaction ($\Delta[R]_{R\rightarrow D}$) was compared to its formation in the thermal process ($\Delta[R]_{D\rightarrow R}$). The ratio $\Delta[R]_{D\rightarrow R}/\Delta[R]_{R\rightarrow D}$ was close to 0.5 for all experiments. Therefore the following balance reaction scheme may be proposed:

$$2H_2Pt \xrightarrow{h\nu} (H_2Pt)_2 \quad (1)$$

$$(H_2Pt)_2 + H_2O \xrightarrow{k} H_2Pt + H_2Pt{-}H_2O \quad (2)$$

where $(H_2Pt)_2$ and H_2Pt-H_2O represent the corresponding dimer(s) and P1, respectively.

Table 1 First-order rate constants of the thermal degradation of the photodimers of H_2Bip and H_2Nep (standard deviations below 10% in all cases)

		k/M^{-1} s^{-1}	
		21 °C	37 °C
H_2Nep	P2	0.0069	0.027
	P3	0.0043	0.020
H_2Bip	P2	0.0069	0.031
	P3	0.0036	0.020

Under the experimental conditions used, disappearance of the dimers and formation of P1 and the reactant followed in all cases first-order kinetics. The corresponding first-order rate constants of the thermal degradation of the dimers (reaction (2)) were determined. Each solution was irradiated 6 min and was then incubated at 21 °C and 37 °C and the consumption of the dimers was monitored as a function of time by means of HPLC analysis. The values of k were calculated from the equation corresponding to first order decays:

$$\ln([D]/[D]_0) = -kt \quad (3)$$

where $[D]_0$ is the initial concentration of a given dimer (immediately after interrupting the irradiation) and [D] is the dimer concentration at time t. The ratio $[D]/[D]_0$ was calculated from the corresponding ratio of areas of the chromatographic peaks of the dimers (A/A_0 at 270 nm). The k values were calculated for P2 and P3, under aerobic and anaerobic conditions (Table 1). It is worth mentioning that, for a given compound, the values corresponding to P2 and P3 are only slightly different. Therefore, although P2 and P3 appear to be isomeric dimers with different chromatographic mobilities, their reactivities are quite similar. As expected, k values increase with incubation temperature (Table 1).

3.3 ^{1}H-NMR analysis of the photodimerization and thermal stability of the dimers

The photodimerization of H_2Bip and H_2Nep and the thermal decomposition of the corresponding dimers in neutral aqueous solutions were also monitored by ^{1}H-NMR in an attempt to characterize in more detail the structural changes occurring during these processes. D_2O was used as a solvent. The ^{1}H-NMR spectra of the non-irradiated solutions of H_2Bip and H_2Nep are given in the experimental part (see also Fig. 1S, ESI‡). The spectrum obtained for H_2Nep is in agreement with literature data.[22]

The H_2Bip and H_2Nep solutions were irradiated during different times and ^{1}H-NMR spectra were registered immediately after interrupting the irradiation. In agreement with the results presented above, all the signals corresponding to the reactants were lower than those registered before irradiation, indicating photochemical consumption of H_2Bip (Fig. 3 and 4) and H_2Nep. In addition, several new signals were detected corresponding to the (photo)products.

The irradiated solutions of H_2Bip and H_2Nep were kept in the dark and the ^{1}H-NMR spectra were registered at different times after irradiation. The signals of photoproducts may be divided into two groups according to the evolution of their intensity in the dark: the intensity of one group of signals decreased with time, whereas the intensity of the other group became more

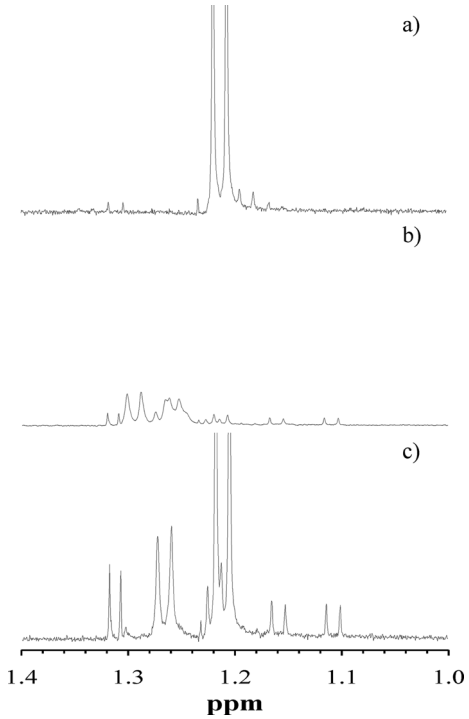

Fig. 3 ^{1}H-NMR spectra of an H_2Bip solution in D_2O (methyl groups): (a) before irradiation; (b) immediately after 20 min of irradiation (at 350 nm); (c) after 20 min of irradiation and 3 h in the dark.

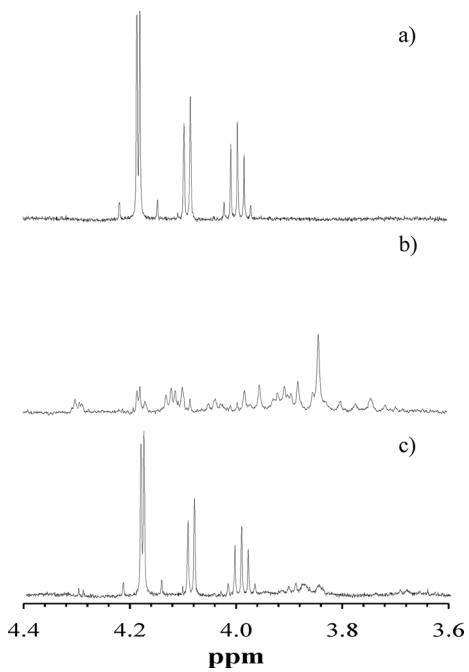

Fig. 4 ^{1}H-NMR spectra of an H_2Bip solution in D_2O between 3.6 and 4.4 ppm: (a) before irradiation; (b) immediately after 20 min of irradiation (at 350 nm); (c) after 20 min of irradiation and 3 h in the dark.

Table 2 Calculated heats of formation and dipole moments of the four possible structures of the photodimers formed by [2 + 2]-cycloaddition of H_2Bip with its 5,8-dihydro tautomer (Scheme 1)

Dimer	Heat of formation (kcal mol^{-1})	Dipole moment (D)
Anti-Ranti	−173.057	4.971
Anti-Rtrans	−170.2680	7.296
Syn-Rsyn	−174.148	9.460
Syn-Rcis	−152.684	9.376

intense. The former group was therefore attributed to the dimers and the latter was assigned to the product(s) of the thermal degradation of the dimers. In addition, as expected taking into account the concentration profiles obtained after irradiation (*vide supra*), the signals corresponding to H_2Bip and H_2Nep increased as a function of the elapsed time in the dark (Fig. 3c and 4c). As H_2Bip exhibits a spectrum easier to interpret than that of H_2Nep, the discussion below is focused on the former case, the two compounds behaving similarly.

^{1}H-NMR analysis of the photodimers. The ^{1}H-NMR spectra of the dimers showed patterns similar to those of the reactants (but with shifts in the corresponding δ values). Typically, in the case of H_2Bip, protons of CγH_3 of the two aliphatic chains of the photodimers give four doublet signals of equivalent intensities that may be attributed to two different dimers, but the small differences in their δ values do not allow specific assignments to each particular dimer (Fig. 3b). These results are in good agreement with the two peaks detected by HPLC (*vide supra*). Likewise, the concentrations of the two dimers, evaluated through the integrated area of the corresponding NMR peaks, were very similar.

Different hypotheses may be formulated on the mechanism of formation of the dimers and their nature. A simple bimolecular process in which two molecules of H_2Pt, one in the excited state and the other in its ground state, react with each other, was discarded by recent evaluations of the quantum yields of photodimerization of H_2Nep (3.8×10^{-2})[21] and H_2Bip (5.3×10^{-2})[20] at an early stage of the reaction. Indeed, quantum yields did not depend on the initial concentration of H_2Pt in a wide range, suggesting that photoisomerization/phototautomerization should occur prior to dimerization.[21] The very reactive 5,8-dihydro tautomer (5,8-H_2Pt) has been reported to be photochemically formed from different pterin derivatives.[23,24] A [2 + 2]-cycloaddition of (7,8-)H_2Pt with its tautomer 5,8-H_2Pt (Scheme 1) might occur through the C9═C10 bonds at the junction of the pyrazine and pyrimidine rings, as suggested for thymine and uracil (pyrimidine derivatives).[25,26] In this case, a signal corresponding to an olefinic proton would be expected in the δ(H) range of ~8–6 ppm in the resulting dimer(s). However, such a signal was not observed.

An alternative hypothesis consists in the [2 + 2]-cycloaddition involving the N5═C6 bond of the reactant (H_2Pt) and the C6═C7 bond of the pyrazine ring of 5,8-H_2Pt. In this case, an azacyclobutane ring would be formed. Four dimers may be theoretically obtained: (i) *syn* or *anti* combinations of the pteridinic moieties on the azacyclobutane, and (ii) for each *syn* or *anti* dimer, the *head-to-head* (*h*,*h*) and *head-to-tail* (*h*,*t*) isomers relative to the position of the carbonyl groups in the pyrimidine

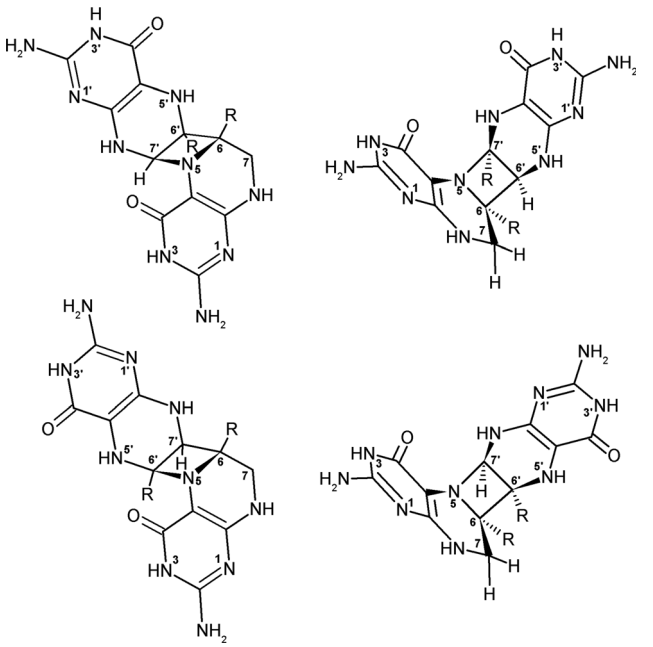

Scheme 2 Structures of the four dimers that may be formed by photodimerization of H_2Bip and H_2Nep. Left: dimers *anti-Rtrans* (top) and *anti-Ranti* (bottom); right: dimers *syn-Rsyn* (top) and *syn-Rcis* (bottom).

rings are possible (Scheme 2). As a consequence, the two aliphatic chains R on the azacyclobutane are in different positions in the four dimers: in two of them, the R groups are on C atoms in position-1,3 relative to each other leading to *anti-Ranti* and *syn-Rsyn* dimers; in the other two dimers, the R chains are on vicinal C atoms leading to *anti-Rtrans* and *syn-Rcis* dimers (Scheme 2, *anti-Rtrans* and *syn-Rsyn* dimers). For the four dimers, heats of formation and dipolar moments were calculated (Table 2). Because of its higher heat of formation and steric hindrance, the *syn-Rcis* dimer may be discarded. However, the small differences between the heats of formation do not allow discrimination between the other three dimers. Moreover, the differences between the dipole moments in the three possible pairs are large enough (>2 D, Table 2) to explain the gap in retention times observed in HPLC.

A detailed analysis of the ^{1}H-NMR spectra in the 3.8–4.0 ppm region (Fig. 4) is in agreement with dimeric structures containing methylene and/or methine protons attached to a tetrahydropyrazine-like structure (THP).[27,28] Actually, in the structures proposed, one THP moiety contains a methylene group ($H_2$7) while the other THP moiety shows a methine proton at C(7′) at the junction with the azacyclobutane (H7′, Scheme 2). The analysis of the relative intensities of growing and decreasing signals points out towards an $H_2$7 broadened singlet in the two dimers (at ~3.84 ppm compared to ~4.2 ppm in H_2Bip). In addition, two new singlet signals were observed with δ values of 3.88 (*s*) and 3.95 (*s*) that may be attributed to the methine proton (H7′) in each dimer (Scheme 3). Moreover, the methine protons of the Cα of the aliphatic chains appeared as doublets, whereas those of the Cβ appeared as multiplets as expected (Scheme 3).

The ^{1}H-NMR spectra do not allow to discriminate between the 3 possible dimers. However, a driving force for the preferential formation of a given dimer might be the existence of

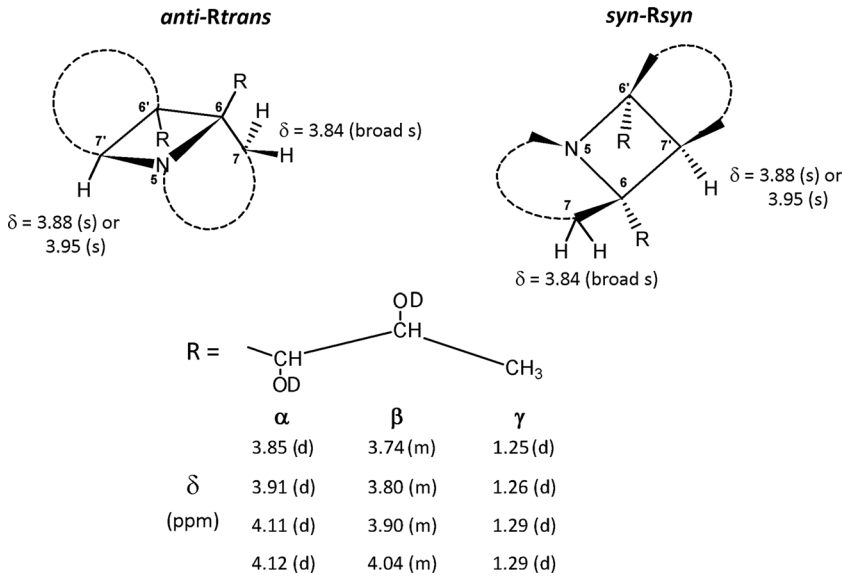

	α	β	γ
	3.85 (d)	3.74 (m)	1.25 (d)
δ	3.91 (d)	3.80 (m)	1.26 (d)
(ppm)	4.11 (d)	3.90 (m)	1.29 (d)
	4.12 (d)	4.04 (m)	1.29 (d)

Scheme 3 Chemical shifts (δ, ppm) of the protons of the azacyclobutane ring and of the aliphatic chains in the two most probable dimers formed by photolysis of H_2Bip in D_2O.

H-bonds between the OH groups of the two aliphatic chains that may favor a previous orientation of the reactants before cyclization and/or stabilize the structure formed. Such an H-bond is possible in the *syn-Rsyn* dimer with the involvement of the OH groups on the Cα atom of each chain, leading to a dissymmetry in the environment of the protons on Cβ. For the *anti-Rtrans* dimer, the H-bonds would be possible between one OH group on the Cβ atom and the other on the Cα′, as well as between the OH group on the Cβ atom of one THP moiety and the HN5 of the other THP. In the case of the *anti-Ranti* dimer however, no H-bond is possible between the aliphatic chains.

In summary, in the case of H_2Bip, taking into account the different arguments presented above, we propose that the most probable structures for the photodimers are *anti-Rtrans* and *syn-Rsyn* (Schemes 2 and 3).

^{1}H-NMR analysis of the thermal stability of the photodimers. ^{1}H-NMR spectra further support the hypotheses made above: even under anaerobic conditions, dimers are unstable and undergo a thermal reaction yielding the original reactant (*i.e.*, H_2Bip or H_2Nep) together with new hydrated compounds (Hyd). Indeed, during their thermal decomposition, a partial recovery of the ^{1}H-NMR signals corresponding to the reactant (H_2Bip or H_2Nep) was observed (Fig. 3 and 4), again in agreement with the concentration profiles obtained by HPLC. Apart from the signals of the reactant, two sets of new signals were registered, therefore pointing out to the formation of two different Hyd (Hyd1 and Hyd2). Therefore the cleavage of the azacyclobutane ring would involve a retro [2 + 2]-cycloaddition where one of the THP moieties gives back the reactant and the other ("photo-tautomer" moiety) undergoes a hydrolysis process incorporating a H_2O molecule.

In the case of polycyclic compounds formed by photodimerization of endocyclic and/or exocyclic alkenes and aza-alkenes, thermal stability of azacyclobutane dimers formed through the [2 + 2]-photocycloaddition depends strongly on stereo-electronic factors as well as on tension induced in the cyclic structures.[29]

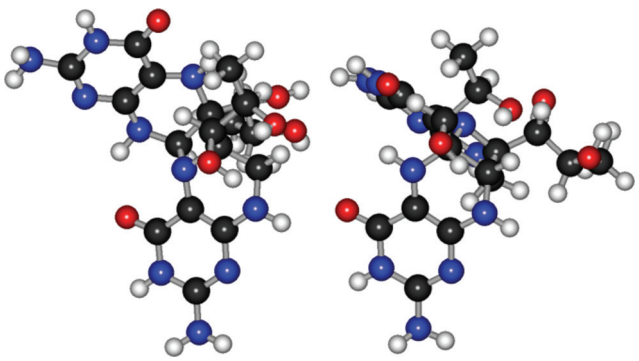

Scheme 4 Examples of rotamers of the two most probable dimers formed by photodimerization of H_2Bip: *left*: dimer *anti-Rtrans* and *right*: dimer *syn-Rsyn*.

The chemical nature and size of the substituents present on the azacyclobutane surrounding region modulate this property. In the present case, the tension induced in the pteridinic moieties when change of hybridization of carbon atoms involved in the azacyclobutane takes place (sp2 to sp3) would account for the thermal decomposition observed, as a common property of all the dimers formed. This would be the first level of control of the retro [2 + 2]-cycloaddition process. This level of thermal stability control is imparted through the structure itself. In addition, the presence of a heteroatom in the azacyclobutane structure would also account for the retro [2 + 2]-cycloaddition process. Furthermore, the size of the polyalcohol chains present as substituent in the C6 position (Scheme 1, H_2Nep, R = –$(CHOH)_2$–CH_2OH and H_2Bip, R = –$(CHOH)_2$–CH_3) would account, because of steric reasons, for the thermal decomposition of the dimers too. This would be a second level of control of the thermal decomposition process suffered by these dimers. Examples of structures of rotamers for the *anti-Rtrans* and *syn-Rsyn* dimers formed from H_2Bip are shown in Scheme 4. The approach of the R substituents and their spatial interaction may be observed.

It is worth mentioning that the two hydrated compounds (Hyd1 and Hyd2) found for a given dihydroderivative are generated in different proportions. Analyzing aliphatic or methyl protons of H_2Bip, at least two groups of signals corresponding to Hyd1 and Hyd2 were registered at 1.22 ppm (d, J = 6.5 Hz) and 1.27 ppm (d, J = 6.5 Hz) (Fig. 3). The concentrations, evaluated through the integrated area of the aliphatic ^{1}H-NMR peaks, yield ~75% and ~25% for Hyd2 and Hyd1, respectively. Therefore when hydrolysis takes place, the two possibilities for the incorporation of the OH group (on C6′ or C7′, Scheme 2) do not occur to the same extent. The asymmetric character of the azacyclobutane ring and the higher steric hindrance on C6′ that bears the aliphatic chain might account for this result.

4 Conclusion

We have investigated in detail the [2 + 2]-photodimerization of 7,8-dihydrobiopterin (H_2Bip) and 7,8-dihydroneopterin (H_2Nep) in neutral aqueous solutions upon UV-A irradiation (320–400 nm). The analysis of the solutions, before and after irradiation, by HPLC coupled to a high resolution mass spectrometer (HRMS, electrospray ionization) confirmed that the two main photoproducts (two HPLC peaks) are isomeric dimers. Moreover, the formation of a product with a different HPLC retention time and a molecular mass corresponding to that of [H_2Pt+H_2O] suggested that dimers were unstable, in the absence as well as in the presence of O_2, and might decompose in the dark by incorporating an H_2O molecule.

Monitoring the evolution of the solutions by ^{1}H-NMR in D_2O confirmed the HPLC and mass spectrometry results and gave new insights into the structural changes occurring both under irradiation and during further reaction in the dark. ^{1}H-NMR data are in agreement with the hypothesis of a [2 + 2]-cycloaddition involving the N5═C6 bond of the reactant (H_2Pt) and the C6═C7 bond of the pyrazine ring of its photo-tautomer 5,8-H_2Pt. Among the four dimers that may result from the formation of the azacyclobutane ring during dimerization, the *syn-Rcis* dimer was discarded on the basis of its higher heat of formation and steric hindrance between the two R aliphatic chains in *cis*-position on vicinal carbon atoms. Calculations of heats of formation and dipole moments did not allow however to discriminate between the other three dimers. Tentative assignments of the two dimers actually formed to the *anti-Rtrans* and *syn-Rsyn* configurations are proposed, taking into account the possibility of a favorable previous orientation and/or a better stabilization of these structures by the formation of H-bonds.

^{1}H-NMR spectra evolution in the dark also show that the dimers are unstable and undergo a thermal decomposition process consisting in a retro [2 + 2]-cycloaddition involving cleavage of the azacyclobutane ring. In this process, one of the tetrahydropyrazine moieties gives back the reactant (with recovery of its ^{1}H-NMR signals) and the other ("tautomer" moiety) undergoes a hydrolysis process incorporating a H_2O molecule. Two hydrolysis compounds were found in the case of both H_2Bip and H_2Nep and were generated in different proportions, as might be expected from the asymmetric character of the azacyclobutane ring and steric factors.

Acknowledgements

The present work was partially supported by Consejo Nacional de Investigaciones Científicas y Técnicas (CONICET-Grant PIP 112-200901-00425 and PIP 00400), Agencia de Promoción Científica y Tecnológica (ANPCyT Grants PICT 33919 and PICT 06-1482), Universidad Nacional de La Plata (UNLP Grant X586) and Universidad de Buenos Aires (Grant 20020100100088). M.V. thanks CONICET for graduate research fellowships. F.M.C., C.L., R.E.B. and A.H.T. are research members of CONICET. C.L., A.H.T., M.V., and E.O. thank Ministerio de Ciencia, Tecnología e Innovación Productiva (MinCyT, Argentina) and ECOS-Sud (France) for financial support of their cooperation project A07E07. The authors thank Jean-Christophe Garrigues (Laboratoire des IMRCP) and Catherine Claparols (Service Commun de Spectrométrie de Masse (FR2599), Université Paul Sabatier (Toulouse III)) for their valuable technical support and helpful discussions of HPLC-MS experiments.

References

1 D. J. Brown, *The Chemistry of Heterocyclic Compounds*, John Wiley & Sons, New York, 1988, pp. 1–42.
2 W. Pfleiderer, *Chemistry and Biology of Pteridines and Folates*, Plenum Press, New York, 1993, pp. 1–16.
3 T. J. Kappock and J. P. Caradonna, Pterin-dependent amino acid hydroxylases, *Chem. Rev.*, 1996, **96**, 2659–2756.
4 E. R. Werner, G. Werner-Felmayr, D. Fuchs, A. Hausen, G. Reibnegger, J. J. Yim, W. Pfleiderer and H. Wachter, Tetrahydrobiopterin biosynthetic activities in human macrophages, fibroblasts, THP-1 and T24 cells. GTP-cyclohydrolase I is stimulated by interferon gamma, and 6-pyrovyl tetrahydropterin synthase and sepiapterinreductase are constitutively present, *J. Biol. Chem.*, 1990, **265**, 3189–3192.
5 C. Huber, J. R. Batchelor, D. Fuchs, A. Hausen, A. Lang, D. Niederwieser, G. Reibnegger, P. Swetly, J. Troppmair and H. Wachter, Immune response-associated production of neopterin. Release from macrophages primarily under control of interferon-gamma, *J. Exp. Med.*, 1984, **160**, 310–316.
6 C. Huber, D. Fuchs, A. Hausen, R. Margreiter, G. Reibnegger, M. Spielberger and H. Wachter, Pteridines as a new marker to detect human T cells activated by allogeneic or modified self major histocompatibility complex (MHC) determinants, *J. Immunol.*, 1983, **130**, 1047–1050.
7 D. Fuchs, G. Weiss and H. Wachter, The role of neopterin as a monitor of cellular immune activation in transplantation, inflammatory, infectious, and malignant diseases, *Crit. Rev. Clin. Lab. Sci.*, 1992, **29**, 307–341.
8 D. Fuchs, G. Weiss and H. Wachter, Neopterin, biochemistry and clinical use as a marker for cellular immune reactions, *Int. Arch. Allergy Immunol.*, 1993, **101**, 1–6.
9 D. Fuchs, A. Hausen, G. Reibnegger, E. R. Werner, M. P. Dierich and H. Wachter, Neopterin as marker for activated cell mediated immunity, *Immunol. Today*, 1988, **9**, 150–155.
10 C. A. Nichol, G. K. Smith and D. S. Duch, Biosynthesis and metabolism of tetrahydrobiopterin and molybdopterin, *Annu. Rev. Biochem.*, 1985, **54**, 729–764.
11 K. U. Schallreuter, G. Büttner, M. R. Pittelkow, J. M. Wood, N. N. Swanson and C. Korner, Regulation of melanin biosynthesis in the human epidermis by tetrahydrobiopterin, *Biochem. Biophys. Res. Commun.*, 1994, **204**, 43–48.
12 K. U. Schallreuter, J. Moore, J. M. Wood, W. D. Beazley, E. M. Peters, L. K. Marles, S. C. Behrens-Williams, R. Dummer, N. Blau and B. Thöny, Epidermal H_2O_2 accumulation alters tetrahydrobiopterin ($6BH_4$) recycling in vitiligo: Identification of a general mechanism in regulation of all $6BH_4$-dependent processes?, *J. Invest. Dermatol.*, 2001, **116**, 167–174.
13 K. U. Schallreuter, J. M. Wood, M. R. Pittelkow, M. Gütlich, K. R. Lemke, W. Rödl, N. N. Swanson, K. Hitzemann and I. Ziegler,

Regulation of melanin biosynthesis in the human epidermis by tetrahydrobiopterin, *Science*, 1994, **263**, 1444–1446.
14 H. Rokos, W. D. Beazley and K. U. Schallreuter, Oxidative stress in vitiligo: Photo-oxidation of pterins produces H_2O_2 and pterin-6-carboxylic acid, *Biochem. Biophys. Res. Commun.*, 2002, **292**, 805–811.
15 A. H. Thomas, C. Lorente, A. L. Capparelli, C. G. Martínez, A. M. Braun and E. Oliveros, Singlet oxygen ($^1\Delta_g$) production by pterin derivatives in aqueous solutions, *Photochem. Photobiol. Sci.*, 2003, **2**, 245–250.
16 M. L. Dántola, M. Vignoni, C. González, C. Lorente, P. Vicendo, E. Oliveros and A. H. Thomas, Electron transfer processes induced by the triplet state of pterins in aqueous solutions, *Free Radical Biol. Med.*, 2010, **49**, 1014–1022.
17 M. Vignoni, F. M. Cabrerizo, C. Lorente and A. H. Thomas, New Results on the Photochemistry of Biopterin and Neopterin in Aqueous Solution, *Photochem. Photobiol.*, 2009, **85**, 365–373.
18 K. Ito and S. Kawanishi, Photoinduced hydroxylation of deoxyguanosine in DNA by pterins: Sequence specificity and mechanism, *Biochemistry*, 1997, **36**, 1774–1781.
19 G. Petroselli, M. L. Dántola, F. M. Cabrerizo, A. L. Capparelli, C. Lorente, E. Oliveros and A. H. Thomas, Oxidation of 2′-Deoxyguanosine 5′-Monophosphate Photoinduced by Pterin: Type I *versus* Type II Mechanism, *J. Am. Chem. Soc.*, 2008, **130**, 3001–3011.
20 M. Vignoni, F. M. Cabrerizo, C. Lorente, C. Claparols, E. Oliveros and A. H. Thomas, Photochemistry of dihydrobiopterin in aqueous solution, *Org. Biomol. Chem.*, 2010, **8**, 800–810.
21 M. Vignoni, M. P. Serrano, E. Oliveros and A. H. Thomas, Photodimerization of 7,8-dihydroneopterin in aqueous solution under UV-A irradiation, *Photochem. Photobiol.*, 2011, **87**, 51–55.
22 Y. Wang, Y. Li, Y. Wu and H. Yan, Mechanism of dihydroneopterin aldolase NMR, equilibrium and transient kinetic studies of the *Staphylococcus aureus* and *Escherichia coli* enzymes, *FEBS J.*, 2007, **274**, 2240–2252.
23 M. L. Dántola, A. H. Thomas, E. Oliveros and C. Lorente, Visible-light photochemistry of 6-formyl-7,8-dihydropterin in aqueous solution, *J. Photochem. Photobiol., A*, 2010, **209**, 104–110.
24 M. Vignoni, M. L. Salum, R. Erra-Balsells, A. H. Thomas and F. M. Cabrerizo, ^{1}H NMR characterization of the intermediate formed upon UV-A excitation of biopterin, neopterin and 6-hydroxymethylpterin in O_2-free aqueous solutions, *Chem. Phys. Lett.*, 2010, **484**, 330–332.
25 B. H. Jennings, S. C. Pastra and J. L. Wellington, Photosensitized dimerization of thymine, *Photochem. Photobiol.*, 1970, **11**, 215–226.
26 B. H. Jennings, S. Pastra-Landis and J. W. Lerman, Photosensitized dimerization of uracil, *Photochem. Photobiol.*, 1972, **15**, 479–491.
27 M Poe and K. Hoogsteen, 5,6,7,8-tetrahydrofolic acid. Conformation of the tetrahydropyrazine ring, *J. Biol. Chem.*, 1978, **253**, 543–546.
28 A. R. Katritzky, N. G. Akhmedov, E. M. Myshakin, A. K. Verma and C. D. Hall, Low-temperature ^{1}H and ^{13}C NMR Spectra of N-Substituted 1,2,3,4-Tetrahydropyrazino[1,2-a]indoles, *Magn. Reson. Chem.*, 2005, **43**, 351–358.
29 T. L. Gilchrist, *Heterocyclic Chemistry*, 3rd edn, Prentice Hall, 1997.